Surficial Geologic Map and Geodatabase of the Cuddeback Lake 30' x 60' Quadrangle, San Bernardino and Kern Counties, California

By Lee Amoroso and David M Miller

Pamphlet to accompany
Open-file Report 2006-1276

2006

U.S. Department of the Interior
U.S. Geological Survey

Surficial geologic map and geodatabase of the Cuddeback Lake 30’ x 60’ quadrangle, California

Abstract

A USGS surficial geologic mapping project, focused on the arid Southwest USA, conducted mapping and process studies to investigate landscape development and tectonic evolution. This project included the Cuddeback Lake 1:100,000-scale quadrangle located in the western Mojave Desert north-northeast of Los Angeles, between the southern Sierra Nevada and San Bernardino Mountains, in Kern and San Bernardino Counties, California. Geomorphic features include high-relief mountains, small hills, volcanic domes, pediments, broad alluvial valleys, and dry lakes. The mapped area includes pre-Tertiary plutonic, metavolcanic, metasedimentary, and other metamorphic rocks; Tertiary sedimentary and volcanic rocks; and Quaternary sediments and basalts. Included in the area are the El Paso, Lockhart, Blackwater, and Muroc faults as well as the central segment of the Garlock fault zone. The tectonically active western Mojave Desert and the variety of surficial materials have resulted in distinctive geomorphic features and terrains.

Geologic mapping has shown that active faults are widespread and have influenced drainage patterns. The tectonically active area near the Garlock fault zone and the nearby El Paso fault influenced development of drainage networks; base level is controlled by fault offset. There is evidence of a late Tertiary drainage network preserved in remnants of alluvial fans and paleo-drainage deposits north of the El Paso Mountains, west of the Lava Mountains, and south and west of the Rand Mountains. Faults identified as being active during the Holocene based on displaced stream channels, scarps, and shutter ridges include the Cantil Valley, Lockhart, Garlock, and Rand Mountain faults. Previously unmapped Holocene and late Pleistocene fault strands identified near the Rand Mountains may represent a splay at the northwest termination of the Lockhart fault. The informally named Grass Valley fault, northwest of Black Mountain, is a right-lateral strike-slip fault that may be a splay of the Blackwater fault. Holocene activity on the Grass Valley fault is indicated by one displaced early Holocene stream terrace. Mapped faults in Fremont Valley are tentatively identified as surficial expressions of the buried Cantil Valley fault.

Introduction

The Cuddeback Lake quadrangle is located in the western Mojave Desert within the Basin and Range physiographic province. The Cuddeback Lake quadrangle lies between longitudes 117° and 118° west and latitudes 35° and 35° 30’ north. Surficial geologic mapping was performed using a combination of aerial-photographic interpretation and on-ground mapping and site visits on all publicly accessible patented and public land. Restricted areas of China Lake Naval Weapons Center and U.S. Air Force Cuddeback Gunnery Range areas were mapped by photo-interpretation only.

The mapping concentrated on areas with late Tertiary and Quaternary deposits. Much of the area is low-relief desert that surrounds small mountains and bedrock knolls and hills. The region is marked by interior drainage; major and minor drainages empty into large playas including Cuddeback Lake, Koehn Lake, and Harper Lake. All these topographic depressions show evidence of tectonic control on their orientation and shape. Small playas are found along faults having a vertical component of displacement that affects drainage patterns.

The climate is arid and exhibits a wide range of daily and seasonal temperature variation. Maximum summer temperatures regularly exceed 38° C while the low winter temperature is about - 8° C. Precipitation primarily comes from Pacific frontal storms; summer rains are infrequent. The western Mojave Desert region is not greatly affected by monsoonal wind shifts and accompanying convection-driven storms (Rowlands, 1995).

Geologic setting

The western Mojave Desert region is tectonically a great triangular fault block, defined by Hewett (1954a) as the Mojave block. This block is bounded by the left-lateral Garlock fault that trends northeast through the upper portion of the Cuddeback Lake quadrangle and separates the Mojave block (to the south) from the Sierra Nevada to the north, and the Great Basin to the northeast. The Mojave block is bounded to the south by the right-lateral San Andreas fault zone. The Mojave block is subdivided by numerous, discontinuous late Cenozoic strike-slip faults that was named the Mojave strike-slip province (Miller and Yount, 2002); a smaller part of the Mojave block was termed the eastern California Shear Zone by Dokka and Travis (1990). The Lockhart, Gravel Hills-Harper Lake, and the Blackwater faults, discussed in the neotectonics section, are in the western part of the Mojave strike-slip province. The faults and many of the physiographic features discussed in this report are identified on Figure 1.

The pre-Quaternary geology is comprised of pre-Tertiary mafic and felsic crystalline and metamorphic rocks, and Tertiary sedimentary and volcanic rocks. The pre-Quaternary materials control erosion and weathering rates, relief and grain size of Quaternary deposits and are therefore classified into groups. Dibblee (1967) classified the pre-Tertiary crystalline and metamorphic rocks into four broad categories. High-pressure/temperature regime metamorphic rocks are mostly Paleozoic and Precambrian schist, mylonite, and gneiss found in the El Paso and eastern Rand Mountains and the Buttes area (Cox and Diggles, 1986; Glazner et al., 1994). Metasedimentary rocks that include marble, phyllite, chert, quartzite, and conglomerate are found in the eastern El Paso Mountains and the Buttes area (Carr et al., 1997; Cox and Diggles, 1986; Fletcher et al., 2002). Shallow-depth intrusive rocks and metavolcanic rocks, mainly coarse to fine-grained, are found in the El Paso Mountains. Plutonic rock types dominated by widely distributed Mesozoic granite also include the Jurassic granite in the western and far eastern parts of the El Paso Mountains and Cretaceous granite north of the Summit Range.

Tertiary sedimentary rocks are mainly continental conglomerate, sandstone, shale and carbonate rock. Tertiary sedimentary deposition was extensive in the El Paso basin. Tertiary rocks (Goler Formation and Ricardo Group) unconformably overlie the plutonic and metamorphic rocks along the north side of the El Paso Mountains and were gently tilted to the northwest between the middle Paleocene and early Miocene (Loomis and Burbank, 1988). There are thick deposits of Tertiary sedimentary rocks in the area northeast of the Lava Mountains. Tertiary volcanic rocks in the Lava Mountains area include silicic tuff and breccia, and rhyolite to basalt lava flows and plugs. Widespread Tertiary volcanism, mainly mafic, extrusive rocks, occur to the east, south, and southeast of the Lava Mountains and the Red Mountain area (Smith et al., 2002). Small Tertiary mafic eruptive centers overlie Tropico Group sedimentary rocks (Miocene) in the southwestern part of the quadrangle (Dibblee, 1967).

Quaternary sediments are the most areally extensive deposits found in the Cuddeback Lake quadrangle; they are distributed from the desert floor to high mountain slopes. Alluvium and colluvium, derived from the hills and mountains, mantle the hillslopes and piedmont areas. Holocene and Pleistocene alluvial fan and terrace deposits consist of gravel to boulder-size clasts, sand, silt and clay. The distal fans grade into fine-grained valley-axis deposits. In many parts of the quadrangle, thin veneers of late Pleistocene and Holocene eolian sand are found in the modern downwind direction from dry lakes and ephemeral drainages.

Major playas and saline lakes are found in depressions within the quadrangle. Koehn Lake south of the El Paso Mountains within Fremont Valley, Cuddeback Lake south of the Lava Mountains, Harper Lake southwest of Black Mountain, and Superior Lake northeast of Opal Mountain in the Superior Valley. These are all likely tectonically controlled depressions, although some of the bounding faults are obscured by thick alluvial deposits.

Previous work

The geology of the Cuddeback Lake quadrangle area has been studied since 1902. Before 1952, much of the work involved describing the ground-water resources (Thompson, 1929) and mineral resource potential. Pack (1914) looked at the oil potential in the Harper Valley area, Hulin (1925) described the mineral potential and geology of the Randsburg 15-minute quadrangle, and Gale (1946) reported on the Kramer borate district. Geologic maps of several of the 15-minute quadrangles were produced by Dibblee (1952) and Dibblee and Gay (1952). Dibblee published geologic maps and reports of the Saltdale quadrangle (Dibblee, 1952) and geologic maps of the Fremont Peak and Opal Mountain quadrangles (Dibblee, 1968). Hewett (1954 a,b) described the general geology and faults of the Mojave Desert. Jennings, Burnett and Troxell (1962) produced a 1:250:000 geologic map of the Trona sheet that encompasses the Cuddeback Lake quadrangle. Dibblee's Areal Geology, Western Mojave Desert, California

(Dibblee, 1967) includes a comprehensive report and compiled geologic maps of the area north of the San Andreas fault to the town of Inyokern and east to the 117 meridian, more than 18,000 km^2 of the western Mojave Desert Region. Clark (1973) produced maps identifying recent activity on the Garlock and associated faults. Area-specific studies within the mapping area include several studies of the El Paso Mountains area including Loomis (1984), Cox and Diggles (1986) and Carr and others (1997). Work in the Lava Mountains area includes Smith (1964), Keenan (2000), and Smith and others (2002). Fletcher (1994) did a field-based project on large-magnitude extension in the central Mojave metamorphic core complex (the Buttes area), also discussed in Fletcher and others (1995).

Methods

The map, accompanying this pamphlet, was produced using remote sensing interpretation of high-resolution aerial photography and processed Landsat imagery along with field verification of unit classification. Most of the bedrock geology was compiled from previous mapping discussed above. Quaternary surficial deposits were classified using a combination of landform and sedimentology, inset relationships, process geomorphology, height above the modern drainage system, and the degree of pedogenesis. Soil pits, 20-70 cm deep, were excavated or exposures along channel cutbanks were cleaned off to examine the soils and determine pedogenesis-based age estimates. During field visits, data was collected to compare the surficial geology to the observed vegetation cover and species, distribution and amount of anthropomorphic disturbance, biological soil crust cover, particle-size analysis samples, mammal burrow density, and micro-topography. Ground and landscape photography was collected to document the appearance of the area. A calibrated color panel was included in the ground photographs for calibration of remote-sensing imagery.

NEOTECTONICS

Blackwater fault – The 55-km-long Blackwater fault along with the Calico fault form the longest strike-slip fault across the Mojave Desert (Oskin and Iriondo, 2004). The southern end of the Blackwater fault extends to within about 10 km of the Calico fault just north of the Mud Hills where a complex (left?) stepover apparently occurs. In this area, late Pleistocene deposits bear scarps but Holocene deposits do not. However, Reynolds and Fay (1989) reported fossil evidence within a Holocene fissure fill. The northern end of the Blackwater fault terminates within 5 km of the Garlock fault where it may cut Holocene deposits locally (Oskin and Iriondo, 2004). This northwest-striking, right-lateral strike-slip fault shows about 8.5 km of right separation in the Calico Mountains-Mud Hills area (Dokka, 1989). Oskin and Iriondo (2004) used new ages for the Black Mountain basalt, 3.77±0.11 Ma, along with a measured 1.8±0.1 km of displacement of the basalt to yield a long-term slip rate estimate for the Blackwater fault of 0.49±0.04 mm/year. Oskin and Iriondo (2004) concluded that the lack of evidence of Holocene fault rupture plus the evidence of rapid and transitory strain accumulation

(Peltzer et al., 2001) supported the conclusion of a higher near-term seismic hazard posed by the Blackwater fault. We have found no evidence for Holocene ruptures along the Blackwater fault and only a few places where scarps cut late to middle Pleistocene (Qia2); most scarps are rounded and involve middle Pleistocene (Qia3), middle to early Pleistocene (Qoa), and early Pleistocene to Pliocene (QToa) deposits. Faults that cut late Pleistocene deposits lie along the southwest front of the Mud Hills in a position that may indicate a left-stepover to the Harper Lake and Gravel Hills faults, with consequent abandonment of the Blackwater fault.

Cantil Valley fault – The Cantil Valley fault is considered to be a splay of the western Garlock fault segment (Louie and Qin, 1991). The 15-km-long fault has been identified by gravity studies and sub-surface information (Louie and Qin, 1991; Mabey, 1960; Pampeyan et al., 1988). The fault has little surface expression except for a zone of faulting at the northeastern end of Fremont Valley, located near the inferred fault. Pampeyan and others (1988) suggested that Cantil Valley fault and the smaller faults found southwest, south, and southeast of Koehn are probably part of the Garlock fault zone. Holocene deposits are cut by scarps in several places and are inferred in other places where fluvial erosion may have enhanced the scarp. Two small Holocene playas are found near the northeastern end of the presumed fault trace.

El Paso fault – The El Paso fault, located along the linear southern flank of the El Paso Mountains, is a 32-km long down-to-the-south normal fault, and is considered a strand of the Garlock fault (Dibblee, 1952; Loomis and Burbank, 1988). The vertical displacement was estimated by Dibblee (1952) to be about 3,000 m. This fault displays evidence of activity during the Pleistocene and Holocene. Gravelly alluvium derived from the El Paso Mountains and exposed along lower Mesquite Canyon has remained in place with respect to its source for most of the Quaternary (Carter, 1980). This alluvium, of late Pliocene age (Carter, 1994), is tilted up to 13° northwest towards the fault. Normal fault displacement has caused base level changes on the Last Chance Canyon drainage during the Quaternary. Deposits west of Bonanza Gulch show significant vertical separation resulting from the base level fall. Late Pleistocene (Qia) terrace/alluvial deposits are found 15 m and Middle Pleistocene (Qoa) deposits are found 35 m above the active channel. Older Holocene terrace deposits (Qyw) are found 3 m above the active wash. Carter (1980) observed there is no evidence of recent lateral movement on the El Paso fault. However, during a field reconnaissance in a canyon 1.5 km northeast of the town of Garlock, middle to late Pleistocene terrace deposits were observed that show left-lateral displacement along splays of the El Paso fault. No paleoseismic studies of the El Paso fault have been done, but a rough estimate of the vertical slip rate can be made from the Mesquite Canyon observations (Figure 2). The perpendicular distance from the observed 13° dip location (UTM 11S 425739 3917271) to the El Paso fault trace is about 650 m. The modern surface slopes about 4.5 degrees so a total of about 17.5 degrees of rotation has occurred relative to the location of the observed dip. This calculates to roughly 200 m of movement on the normal fault. If fault movement initiated about 2 Mya, during the deposition of the fan alluvium, this yields a slip rate of ~ 0.1 mm/year.

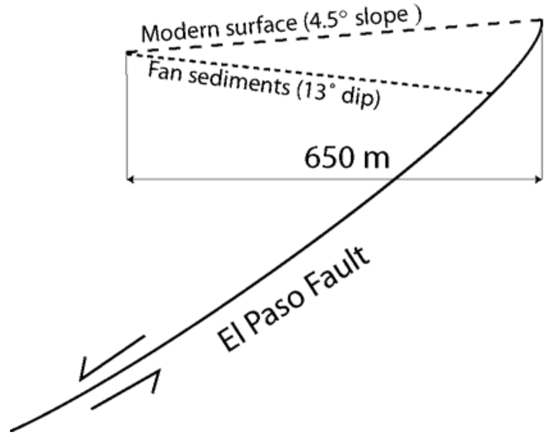

Figure 2. Sketch showing the relation of the present fan surface, the dip of the Pliocene alluvium, and the El Paso fault. The drawing is not to scale, and the actual dip on the fault is not known.

Garlock fault – The Garlock fault is a broadly arcuate zone of northeast striking, mainly left-lateral faults extending 248-km from the San Andreas fault near Ft. Tejon northeast to the southern end of Death Valley. Fault locations were identified by aerial photographic inspection and the literature (Clark, 1973; McGill and Rockwell, 1998; McGill and Sieh, 1991, 1993). An estimated 48 to 74 km of left slip was documented for this fault zone (Carr et al., 1993; Davis and Burchfiel, 1973; Loomis and Burbank, 1988; Michael, 1966). Estimates of initial movement on the Garlock include the early Miocene (Louie and Qin, 1991), late Miocene (Loomis and Burbank, 1988), post-early Miocene (Monastero et al., 1997), and early middle Miocene (Smith et al., 2002); slip has continued into the late Quaternary. The left-lateral displacement sense of the Garlock fault zone is well established (Davis and Burchfiel, 1973; Dibblee, 1952; Dibblee and Gay, 1952; Michael, 1966). In the Cuddeback Lake quadrangle, evidence for left lateral displacement of Holocene alluvial deposits and drainages, as well as Pleistocene terrace deposits and shutter ridges, are well exposed from Goler Gulch to just west of the town of Garlock. Folds associated with the Garlock fault affect Pleistocene surficial deposits east of Red Rock Canyon and northeast of the Lava Mountains where the Christmas Canyon Formation is deformed (Smith, 1991). The Christmas Canyon Formation is attributed by Smith (1991) as being Pleistocene age, but the lack of access to the China Lake Naval Weapons Center precluded field verification.

The formation of Fremont Valley, which created the Cantil basin, is suggested to be the result of a dilatational left stepover on the Garlock fault (Aydin and Nur, 1982; Westaway, 1995). An alternative hypothesis to explain the Cantil Basin extension is a proposed interaction of the Garlock and right-lateral Lockhart-Helendale faults resulting in the counterclockwise rotation of tectonic blocks in the western Mojave Desert (Carter et al., 1987; Louie and Qin, 1991).

The Garlock fault has been divided into segments by McGill and Sieh (1991); the western segment extends west from the Koehn Lake stepover to the San Andreas fault, and central segment extends from that stepover eastward to the Quail Mountains. Slip rate estimates have been made for several locations along the western and central segments. Results from a paleoseismic investigation on the western Garlock fault (just west of the Cuddeback Lake quadrangle) found the early Holocene slip rate to be about 6 mm/yr (McGill et al., 2003). Carter (1980) used displaced gravel fans, 7 km east of Koehn Lake, to estimate a slip rate of about 12 mm/year in the Pleistocene and an average rate of 7-8 mm/year for the Holocene. McGill and Sieh (1991,1993) estimated that the late Pleistocene slip rate in the central Garlock fault segment was ~5 to 7 mm/year.

The Garlock fault has been active throughout the Quaternary. The fault has cut early Pleistocene to late Holocene alluvial fan, playa, and lacustrine deposits from Mesquite Canyon to east of Highway 395. Holocene drainages show left-lateral offset or are blocked by shutter ridges, especially noticeable near Mesquite Canyon. Fault stepovers have created closed basins that are filled with Holocene alluvium.

Grass Valley fault – The Grass Valley fault is the informal name for a 9-km long zone of right-lateral strike-slip faults found along a line of low rhyolite hills west of Grass Valley. The slip sense is shown by offset drainages, beheaded alluvial fans, and offset shutter ridges. This fault displaces QToa, Qoa, Qia, and perhaps Qyao deposits by different amounts, implying tectonic activity throughout the Quaternary. There is an estimated 370 m of right lateral slip based on displacement of a QToa alluvial fan from a large drainage (UTM 11S 466350 3908160). The Grass Valley fault may be a splay of the Blackwater fault but no evidence of linkage of surface rupture can be found between the southeastern end of the rhyolite hills and the small fault strands of the Blackwater fault seen near the north end of Black Canyon.

Harper fault Zone – The Harper fault zone is a zone of shorter, primarily right-lateral strike-slip faults including, from northwest to southeast, the Cuddeback fault, Gravel Hills fault, Harper Valley fault, Harper Lake fault, and the Black Mountain fault.

Cuddeback fault – The 4.5-km long Cuddeback fault was mapped by Dibblee (1968) as a right-lateral strike-slip fault. The fault displaces Tertiary Barstow Formation (Qha/sl) and does not show evidence of Holocene activity.

Gravel Hills fault – The Gravel Hills fault is a 16-km long right-lateral oblique fault with significant up to the northeast vertical displacement (Dibblee, 1968). The amount of strike-slip offset is not well constrained; Dibblee (1968) suggested that the axis of the Gravel Hills syncline has been displaced by ~ 0.8 km. There is evidence of Holocene movement: Displaced Holocene alluvium exists at several places along the Gravel Hills fault northeast of Fremont Peak (e.g. UTM 11S 464260 3894895). There are offset modern channels and a small closed depression containing an active playa that borders the fault.

Harper Valley fault – The Harper Valley fault, southwest of Black Mountain, is a northwest-striking fault with up-to-the-northeast vertical displacement (Dibblee, 1968). This fault offsets a range of geologic units, from Pliocene basalts to Holocene alluvium (e.g. UTM 11S 472048 3888180). Drainages show evidence of gradient changes where they cross the fault. No strike-slip sense of displacement was noted.

Harper Lake fault – The Harper Lake fault is likely the continuation of the Black Mountain fault (Bryant, 1987). South of Black Mountain, several faults form a broad zone within which Pleistocene deposits are cut and early Holocene deposits are folded.

Black Mountain fault – The Black Mountain fault is an approximately 30-km-long northwest-trending zone of high-angle faults, with a right-lateral strike-slip component, mapped by Dibblee (1968). Dibblee (1968) estimated about 0.8-km of right-lateral offset based on displacement of the Black Mountain anticline and as much as 600 m of down-to-the-southwest vertical displacement. The Black Mountain fault displaces the Black Mountain Basalt, which has yielded dates of 2.55±0.58 Ma (Burke et al., 1982) and 3.77±0.11 Ma (Oskin and Iriondo, 2004). There is little evidence of late Pleistocene activity on this fault; Bryant (1987) reported that an old, presumably late Pleistocene shoreline of Harper Lake is not offset by the Black Mountain fault. The Black Mountain fault cuts Qoa and Qia deposits but does not appear to cut Holocene deposits.

Lockhart fault Zone – The Lockhart fault Zone consists of the sub-parallel Lockhart, South Lockhart, and North Lockhart faults. Although surface traces are discontinuous (Dokka and Travis, 1990), map patterns and seismic evidence suggest that the Lockhart fault is a continuation of the Lenwood fault, and the South Lockhart fault is the northwestern extension of the Helendale fault (Dibblee, 1985; Louie and Qin, 1991; Page and Moyle, 1960; Schell, 1994).

Lockhart fault – The 40-km-long right-lateral strike-slip Lockhart fault extends from just west of Barstow to the southern flank of the Rand Mountains. Dibblee (1968) stated that the fault is right-lateral strike-slip but the amount of displacement is not known (Dokka and Travis, 1990). The fault has a down to the northeast component that is most apparent east of Highway 395. Northwest of Highway 395, the fault trace is manifested as a dissected scarp or is aligned with a broad erosional trough (Bryant, 1987). The fault displaces Quaternary alluvium and places Holocene against late Pleistocene deposits east of Highway 395 (Bryant, 1987). The creation of a small mid- to late(?)-Holocene playa (UTM

11S 452350 3882460) due to ~30 cm of uplift that dammed a small drainage suggests this fault has been active during much of the Holocene.

The Lockhart fault splays just west of Highway 395 and creates a small playa near the splay termination (UTM 11S 444700 3892915). The main fault trends farther northwest, becomes discontinuous, and terminates in a broad splay of faults and lineaments near the Rand Mountains. During a paleoseismic trenching investigation Schell (1994) observed that some north and north-northwest trending lineaments mapped on the Rand Mountains pediment appear to be faults exhibiting evidence of Holocene rupture. The north-striking faults and small grabens in the western part of the Rand pediment may also be related to the Lockhart fault zone or may be the result of interaction between the Lockhart fault and normal faults that bound the northern part of the Rand Mountains.

South Lockhart fault – The South Lockhart fault is a 27-km-long north to northwest striking fault. The fault trace is discontinuous and the vertical displacement sense varies from down to the south to down to the north. QToa gravel deposits, located 11 km northwest of the Boron Air Force Station, are found on either side of the fault (UTM 11S 438630 3889500). It appears that these deposits have been offset by a minimum of 1 km since QToa time. There is no evidence of displaced streams along the South Lockhart fault.

North Lockhart fault – The 6-km-long North Lockhart fault was classified as right-lateral strike-slip by Dibblee (1968). This fault shows down-to-the-north vertical displacement near its southeastern end. The fault offsets mid- to late-Pleistocene alluvium and places mid-Pleistocene against Holocene alluvium at the southeastern end of the fault (UTM 11S 459305 3880672).

Muroc fault – The main 8-km-long Muroc fault shows a down to the southwest displacement and places bedrock against late Pleistocene to Holocene(?) grussy alluvium. Subsidiary faults show west-northwest to northeast orientations and several senses of displacement.

Rand Mountains fault zone – The Rand Mountains fault zone is an informally named zone (Pampeyan et al., 1988) of normal faults along the northern, dissected flank of the Rand Mountains. The northeast striking zone of faults places granite against alluvium in the southwest part of the range. Further to the northeast, the faults cut alluvium on the piedmont. Mid- to late-Pleistocene alluvium has been vertically offset down to the north as much as 2.5 m; Holocene offset of alluvial fans is as much as 1.2 m. These faults may not be related to the extension at the stepover of the Garlock fault as they lie outside the overlap zone, which lies further north in the Fremont Valley.

GEOMORPHOLOGY

Late Tertiary to early Quaternary alluvium and its relation to paleo-drainages

A linear, discontinuous pattern for late Tertiary to early Pleistocene alluvial deposits suggests that they represent former drainages. They are classified as paleo-drainages because the deposits are found more than 15 m above the present base level or the deposits lie on bedrock that was not the source of the clasts. The remnants of late Tertiary to early Quaternary (QToa) and a few mid-Pleistocene (Qoa) deposits are found north of the El Paso Mountains, west of the Lava Mountains, and south of the Rand Mountains.

The QToa deposits west of the Lava Mountains consist of rounded clasts of andesite and basalt. The top of the deposit is about 45 m above the present base level. The rounding of the clasts suggests they were fluvially transported westward from a likely Lava Mountains source. Matrix material between the clasts shows significant pedogenesis, with clayey, angular peds. The thickness and topographic expression of the bouldery deposit points to the transport of the clasts within a broad valley of moderate gradient that drained into the Neogene Cantil Basin (Koehn Basin of Dibblee, 1967).

Deposits of imbricated, well-rounded granite and other clasts (QToa gravels) found south of the Rand Mountains and 9 km southwest of Galileo Hill (UTM 11S 422270 3893727) suggest southwest flowing streams that crossed the granite pediment during the late Pliocene (?) and early Pleistocene. The polymict clast assemblage includes several types of coarsely crystalline pink granites and potassium feldspar-rich red granites, lithic tuffs and felsite, andesite, rhyolite, and some basalt. The deposits are generally well cemented with pedogenic carbonate and may have a laminar cap preserved. The soil carbonate has been brecciated and is cross-cut by calcite-filled dikes (Stage IV to V pedogenic carbonate morphology).

In several locations, these polymictic QToa gravels unconformably overlie granodiorite bedrock (e.g. UTM 11S 425242 3893877), in places as channels cut into the bedrock (UTM 11S 425645 3893833), suggesting that these QToa sediments were probably transported over the pediment. Locally derived granodiorite clasts are found in these deposits. Clast imbrication suggests transport was to the southwest and west. The clast types are similar to that of conglomerates in the Goler Formation and Upper Dove Spring Formation and may be reworked from these deposits.

A sinuous deposit of QToa and Qoa alluvium that lies northeast of the State Highway 14 (UTM 11S 411425 3913250), is found on ridge tops that parallel a small drainage that empties into Red Rock Canyon (southeast of the abandoned town of Ricardo). Sub-angular to sub-rounded gravel to cobble-sized clasts of granites, quartzite, andesite, and basalt within a grus matrix unconformably overlie middle Dove Spring Formation rocks. No imbrication or other indicators of flow direction were observed.

Pediments and pediment formation

Pediments are nearly flat erosional surfaces in various stages of bedrock degradation, exposure, and burial. They are formed on granite and granodiorite bedrock in the east-central, south-central, and western parts of the Cuddeback Lake quadrangle. The pediments, whether incised, deeply dissected, or characterized by a veneer of alluvium or weathering products, surround many of the plutonic rock-cored hills and mountains. Pediments have been hypothesized to form by the downwasting of deep (late Tertiary?) weathering horizons and erosion of the weathered materials (Dohrenwend et al., 1986), the backwasting of regolith-covered slopes (Oberlander, 1989), or parallel slope retreat from a bounding fault (Cooke and Warren, 1973).

Observations supporting the downwasting model are seen in the residual hills of granite capped by polymictic QToa alluvium previously described. The QToa allluvial caps, which likely represent late Tertiary to early Quaternary river deposits, are now up to 30 m above the modern drainages. Another location, 10 km southeast of Castle Butte, shows about 10 m of pediment downwasting. This is estimated from the elevation difference of the contact at the base of small basalt hills overlying granite to the modern valley floor.

Pediment formation on the southern part of the western half of the Rand Mountains appears to be tectonically controlled, by either uplift of the mountain block or down dropping of the Fremont Valley. The pediment here has a thin veneer (Qpv, <2 m thick) though northwest of Galileo Hill, the pediment appears to be buried by young grussy alluvium. Pediment formation here likely predates tectonic displacement because the present pediment surface ends abruptly at the mountain crest. The Mabey (1960) gravity map does not show good evidence of a bounding-fault along the southern flank of the Rand Mountains. It appears that the pediment was terminated during the creation of the deep basin beneath Fremont Valley due to movement on the Garlock fault. Based on age estimates of initial movement on the Garlock fault pedimentation may have begun in the western Mojave Desert before early to mid-Miocene time (Louie and Qin, 1991; Monastero et al., 1997; Smith et al., 2002). This observation implies that pedimentation may have started in the western Mojave Desert before pediment dome formation was initiated (late Miocene) in the eastern Mojave Desert (Dohrenwend et al., 1986).

Escarpment backwasting is seen along the Muroc fault, where the topographic crest has retreated approximately 475 m from the fault trace. Smaller amounts of scarp retreat are seen from small fault splays along the Muroc fault trace. Backwasting is also occurring where strands of the Lockhart fault and Southern Lockhart fault cut across granitic pediments. Where there is a dip-slip component of movement, the local topographic crest has retreated from the fault trace.

Development and age of pediment veneers

The relation of soil developed on weathered bedrock and alluvium to pediment development in the Mojave Desert has been studied by several investigators (Boettinger and Southard, 1991, 1995; Cooke and Mason, 1973; Eghbal and Southard, 1993a, b). Because weathered bedrock and saprolite are usually found beneath the alluvial veneer on the pediment (Qpv), it appears that some of the mid- to late-Pleistocene alluvial veneer is developed from locally derived saprolite. That is, the weathering of the in-place bedrock precedes alluviation and the development of soil, an idea proposed by Cooke and Mason (1973). They also asserted that there was ‘no consistent or distinctive relationship between the soil profile and the extent of bedrock weathering’, that is, that the soil formation and bedrock weathering occurred separately. Based on the Boettinger and Southard (1991) work and field observations, the granite saprolite could be the parent material for much of the Qiag and Qoag deposits on granitic pediments in the Cuddeback Lake quadrangle.

Evidence supporting this including preservation of rock fabric, clay chemistry consistent with weathering of the parent material silicates (Boettinger and Southard, 1991), and translocation of soluble minerals and silica deeper within the matrix is seen in many places on the pediment (Qpv) beneath the surface veneer. In contrast, the lack of bedrock fabric, the presence of illuviated materials (clay, silt, and carbonate) or horizontal stratification suggests that soils are being formed in alluvium derived from the eroding of bedrock or exposed saprolite. This is particularly apparent in the Qiag and Qoag deposits located southwest of Fremont Peak and west of The Buttes. The age of these deposits is not well constrained. Eghbal and Southard (1993a,b) looked at the micromorphology and stratigraphy of soils formed in granitic alluvium northeast of California City. This alluvium was probably derived from erosion of the pediment on the south side of the Rand Mountains. These soils (equivalent to Qyag4 to Qiag 2) appear to be developed on reworked, very old alluvium, more than 783 ka because the deeper part of the deposit (> 2m) has a reversed paleomagnetic polarity (Eghbal and Southard, 1993a). This suggests that the Qoag alluvium is older than mid-Pleistocene.

Acknowledgements: This surficial geologic map is a product of the Surficial Geology Project, funded by the National Cooperative Geologic Mapping and Earth Surface Dynamics Programs, U.S. Geological Survey. Reviews by Robert Powell and Geoff Phelps are appreciated for the improvements they brought to the map and map unit descriptions. We appreciate discussions with Mike Oskin, Bob Reynolds, and Brett Cox that helped us to understand several aspects of active tectonics and regional geology.

Descriptions of map units:

Anthropogenic deposits

ml **Made land or artificial fill (latest Holocene) –** Surficial material moved for mining, construction, and agriculture that is extensively disturbed, making landforms and deposits difficult to classify

Qpf **Ponded fill (latest Holocene) –** Sand and silt deposits that are active and have received material in the last few decades as the result of damming of drainages by man-made features such as roads, railroad beds and flood control barriers; similar to **Qap** deposits. Usually vegetated with creosote bush (*Larrea tridentata*) and saltbush (*Atriplex sp.*)

Valley-axis deposits

Qav **Active valley-axis deposit (latest Holocene) –** Loose, fine-grained deposits in valley axes characterized by anastamosing ephemeral washes, low-relief interfluves, and eolian deposits. Small active playa deposits may be associated with these deposits. Prone to flooding, moderately vegetated with various perennial shrubs such as desert senna (*Senna armata*), creosote bush (*Larrea tridentata*), white bur-sage (*Ambrosia dumosa*), and saltbush (*Atriplex sp).* Prone to inundation and flooding during and after heavy rains

Qyv **Young valley-axis deposit (Holocene and latest Pleistocene) –** Deposits of sand to small gravels in valley axis locations characterized by inactive anastamosing ephemeral washes, low-relief interfluves, and eolian deposits. These deposits grade into the distal portions of **Qya** fans. Soil formation is similar to **Qya**. Small young playa deposits may be associated with these deposits. Prone to flooding in heavy rains, moderately vegetated with creosote bush (*Larrea tridentata*), white bur-sage (*Ambrosia dumosa*), and several species of saltbush (*Atriplex sp)*

Wash deposits

Qaw **Active wash deposit (latest Holocene) –** Alluvial wash deposits characterized by surfaces and channels that are active and have received deposits within the last few decades. The deposits are moderately to poorly sorted sand, sandy gravel, and clasts to 80 cm in diameter. Deposits are coarser grained near mountain fronts or where washes cross boulder to cobble-bearing parent materials, alluvium is poorly to moderately bedded and loose. Channel bars up to 50 cm in height. Smaller alluvial wash tracts are generally included in young alluvial fan deposits unit (**Qaa**). This deposit shows little to no soil development. Unit sparsely vegetated with various perennial shrubs such as desert senna (*Senna armata*), creosote bush (*Larrea tridentata*), and white bur-sage (*Ambrosia dumosa*), as well as annuals. Prone to channelized flow and flooding during and after heavy rains. Active on a decadal time scale based on burial of or damage to late 20th Century trails, roads, and structures. Diagnostic features: Narrow, elongate channels that generally increase in width down channel.

Qawg **Active wash deposit composed primarily of grus (latest Holocene) –** Alluvial wash deposits characterized by surfaces and channels that are active and have received deposits within the last few decades. The deposits are moderately to poorly sorted sand and small gravel

Qyw **Young wash deposit (Holocene and latest Pleistocene) –** Moderately to poorly sorted sand and silt, sandy gravel, and clasts to 50 cm in diameter. Deposits are coarser grained near mountain fronts, steep alluvial fans, or where washes cross boulder to cobble-bearing parent materials. Poorly to moderately bedded, loose to poorly consolidated. Channel bars up to 50 cm in height. Smaller alluvial wash tracts are generally designated as younger alluvial fan deposits (**Qya**). Younger deposits show no soil development (similar to **Qya**), older deposits may show weak, incipient Av horizon and weak B horizon development (similar to **Qyao**). Unit sparsely to moderately vegetated with various perennial shrubs including desert senna (*Senna armata*), creosote bush (*Larrea tridentata*), white bur-sage (*Ambrosia dumosa*), and several species of saltbush (*Atriplex sp)*. Prone to channelized flow and flooding during and after heavy rains. Active on a centennial time scale based on burial of late 19th and early 20th Century trails and structures. Diagnostic features: Narrow, elongate geomorphic features that generally increase in width down channel

Qiw **Intermediate-age wash deposit (late and middle Pleistocene) –** Parent material is moderately to poorly sorted sand and silt, sandy gravel, and clasts to 40 cm in diameter. Deposits are coarser grained near mountain fronts and may be up to 5 m above the active channel (up to 8 m near active faults). Poorly to moderately bedded, poorly to moderately consolidated. Channel bars up to 10 cm in height. Younger deposits show no soil development (similar to **Qya**), older deposits may show Av horizons to 3 cm and weak B horizon development (similar to **Qia**). Unit sparsely to moderately vegetated with various perennial shrubs such as creosote bush (*Larrea tridentata*), white bur-sage (*Ambrosia dumosa*), and box thorn (*Lycium sp.)*. Prone to channelized flow and flooding during and after heavy rains. Diagnostic features: Narrow, elongate geomorphic remnant features along larger drainages

Alluvial deposits

Qaa **Active alluvial fan deposit (latest Holocene) -** Alluvial fan deposits characterized by surfaces that are active and have received deposits within the last few decades. Moderately to poorly sorted sand, sandy gravel, and clasts to 25 cm in diameter with little or no soil development. Alluvium has coarser texture near mountain fronts or older coarse-grained deposits that are being reworked; average grain-size decreases downslope. The alluvium is poorly to moderately bedded and loose, channel bars are as high as 30 cm. Qaa deposits lie 10-30 cm above or grade to active channels with few vertical cutbanks, and inset into unit Qya. Unit is sparsely vegetated with various perennial shrubs such as desert senna (*Senna armata*), creosote bush (*Larrea tridentata*), white bur-sage (*Ambrosia dumosa*), and saltbush (*Atriplex sp)*. Prone to inundation and flooding during and after heavy rains. Diagnostic features: Narrow, elongate geomorphic features above, and adjacent to, the active channel

Qya **Young alluvial fan deposit (Holocene and latest Pleistocene) –**Moderately to poorly sorted sand and silt, sandy gravel, and clasts to 85 cm in diameter. Deposits are characterized by abandoned surfaces that receive material infrequently. Poorly bedded to massive, loose to poorly consolidated. Bar and swale micro-topography averages 25 cm in height and decreases down fan. Surfaces lie 10-50 cm above active channels (up to 300 cm near active faults) and may be inset into unit **Qia**. These deposits show little or no soil development. Unit moderately to well vegetated with various perennial shrubs such as desert senna (*Senna armata*), creosote bush (*Larrea tridentata*), white bur-sage (*Ambrosia dumosa*), and several saltbush *(Atriplex sp)*species. Surface may be flooded (up to 25 cm deep based on flotsam evidence) during and after heavy rains. Active on a centennial time scale based on burial of late 19th and early 20th Century trails and structures. Diagnostic features: Terraces along younger to active channels and younger alluvial fans, no pavement or desert varnish development

Qyao **Older young alluvial fan deposit (early Holocene and latest Pleistocene) –** Moderately to poorly sorted sand and silt, sandy gravel, and clasts to 75 cm in diameter. Deposits are characterized by abandoned surfaces that receive material very infrequently. Poorly bedded to massive, loose to weakly consolidated. Bar and swale micro-topography averages 20 cm in height and decreases down fan. Surfaces lie 25-75 cm above active channels (up to 500 cm near active faults) and may be inset into unit **Qia**. These deposits show little to moderate soil development, incipient to weak Av horizons as thick as 3 cm and weak to moderate cambic B horizon development (7.5 YR hue). Little or no desert pavement development. Some late Pleistocene soils have Stage I to I+ pedogenic carbonate morphology. Unit moderately to well vegetated with various perennial shrubs such as creosote bush (*Larrea tridentata*), white bur-sage (*Ambrosia dumosa*), several species of saltbush (*Atriplex sp),* and Mormon tea (*Ephedra nevadensis*). Surface may be infrequently flooded during and after heavy rains. Diagnostic features: Terraces along younger to older channels and older young alluvial fans, none to weak pavement and minor desert varnish development

Qia **Intermediate-age alluvial fan deposit (late and middle Pleistocene) –** Sediments are moderately to poorly sorted sand and silt, sandy gravel, and clasts to 130 cm in diameter. Deposits are characterized by surfaces that have been abandoned for tens to hundreds of thousands of years. Poorly bedded to massive, weakly to moderately consolidated. Bar and swale micro-topography is subdued to 10 cm in height, though the surface is generally flat and incised by shallow channels. Surfaces lay an average of 250 cm above active channels (up to 10 m near active faults) and may be inset into unit **Qoa**. These deposits show moderate to strong soil development, well-developed platy to blocky Av horizons as thick as 8 cm and moderate cambic B horizon development (7.5 to 5 YR hue). Older

Qia deposits have argillic Bt (to 2.5 YR hue) with angular, prismatic peds or may have eroded litter from exhumed calcic horizons. Some mid- to late Pleistocene soils have Stage II to III+ pedogenic carbonate morphology. Unit is sparsely to moderately vegetated with various perennial shrubs such as creosote bush (*Larrea tridentata*), white bur-sage (*Ambrosia dumosa*), and box thorn (*Lycium sp.).* Rhatany (*Krameria grayi*) appears to prefer carbonate-rich soils. Surface is rarely flooded during and after heavy rains. Diagnostic features: Old alluvial fans generally confined to the mountain front, flat surfaces with moderate to strong pavement development and well-developed desert varnish.

Qoa **Old alluvial fan deposit (middle and early Pleistocene) –** Parent material is moderately to poorly sorted sand, sandy gravel, and clasts to 110 cm in diameter. Deposits are characterized by deeply incised fan remnants that have been abandoned for hundreds of thousands of years. Many surfaces have been stripped down to the well-indurated soil carbonate or are littered with carbonate debris. Poorly bedded to massive, well consolidated. Surfaces lay an average of 850 cm above active channels (up to 20 m near active faults) and may be inset into late Tertiary units. These deposits show strong soil development. **Qoa** deposits have Stage IV and greater carbonate morphology. Younger deposits with Av horizons and cambic B horizon may be developed unconformably on the stripped **Qoa** deposit. Unit is sparsely to moderately vegetated with various perennial shrubs such as creosote bush (*Larrea tridentata*), white bur-sage (*Ambrosia dumosa*), and box thorn (*Lycium sp.).* Rhatany (*Krameria grayi*) appears to prefer carbonate-rich soils. Surface is rarely flooded during and after heavy rains. Diagnostic features: Degraded alluvial fans generally confined to the mountain front, forms ballenas that exhibit no to strong pavement, Stage III-VI pedogenic carbonate exposed at the surface

QToa **Extremely old alluvial fan deposit (early Pleistocene and Pliocene) –** Alluvial fan deposits characterized by the degraded remnants of abandoned surfaces. Parent material is moderately to poorly sorted sand, sandy gravel, and clasts to 400 cm in diameter. The lithology of the clasts is predominantly mafic volcanic rocks for QToa units near the Lava Mountains, Almond Mountain, Black Mountain, or Black Hills/El Paso Mountains. QToa deposits south and west of the Rand Mountains have a mixed lithology including several types of granites, quartzites, tuff, glassy rhyolite, plus or minus some andesites and basalts. Poly-lithology QToa deposits are similar to lower Cudahy Camp Formation conglomerates, which in turn are suggested to be reworked Goler Formation (Loomis and Burbank, 1988). The deposits west of Galileo Hill show imbrication implying transport to the southwest. Some of these polymict QToa deposits are found in paleo-channels cut into the granite pediment.

Surfaces are characterized by deeply incised remnants of surfaces that have been abandoned for many hundreds of thousands of years. Surfaces range from rounded remnants to planar landforms up to 50 m above the modern drainages. Many surfaces have been stripped down to the well-indurated soil carbonate or are littered with carbonate debris. Soils may be forming on more recently deposited eolian and alluvial material. Poorly bedded to massive, well consolidated. Unit is sparsely to moderately vegetated with various perennial shrubs such as white bur-sage (*Ambrosia dumosa*) and box thorn (*Lycium sp.).* creosote bush (*Larrea tridentata*) is usually a minor component. Desert Trumpet (*Eriogonum inflatum*) abound on the high planar deposits. Surface is very rarely flooded during and after heavy rains. Diagnostic features: These deposits generally did not form in the present topography, **QToa** depositional geomorphic features appear to be cut off from the original source areas. Generally, the deposits are polymict gravels that overlie an unrelated deposit

Alluvial deposits of grus

Qaag **Active alluvial fan deposit composed of grus (latest Holocene) –** Composed of moderately to poorly sorted sand and fine gravel derived from grus producing granite sources but may contain clasts from other lithologic sources. Surfaces have received deposits within the last few decades. Poorly bedded to massive, loose to very weakly consolidated. These deposits show no soil development. Unit moderately to well vegetated with various perennial shrubs such as creosote bush (*Larrea tridentata*), white bur-sage (*Ambrosia dumosa*), and desert senna (*Senna armata*). Surface may be flooded during and after heavy rains. Drainage patterns are simple, some have low relief that may be related to grain size. Diagnostic features: Terraces along younger to active channels and younger alluvial fans, no pavement or desert varnish development

Qyag **Young alluvial fan deposit composed of grus (Holocene and latest Pleistocene) –** Moderately to poorly sorted sand and fine gravel derived from grus-producing granite sources but may contain clasts from other lithologic sources. Deposits are characterized by abandoned surfaces that receive material infrequently. Poorly bedded to massive, loose to very weakly consolidated. Bar and swale micro-topography usually subdued but may be as high as 20-40 cm near mountain fronts. Surfaces lie 10-30 cm above active channels and may be inset into unit **Qiag**. These deposits show little or no soil development. Unit moderately to well vegetated with various perennial shrubs such as creosote bush (*Larrea tridentata*), white bur-sage (*Ambrosia dumosa*), and several species of saltbush (*Atriplex sp)*. Surface may be flooded during and after heavy rains. Drainage patterns are simple with low relief and may be related to grain size. Diagnostic features: Terraces along younger to active channels and younger alluvial fans, no pavement or desert varnish development

Qyaog **Older young alluvial fan deposits composed of grus (early Holocene and latest Pleistocene) –** Parent material is moderately to poorly sorted sand and silt derived from grus producing granite sources but may contain clasts from other lithologic sources; poorly bedded to massive, loose to weakly consolidated. Surfaces are largely abandoned and receive material infrequently. The bar and swale micro-topography is usually subdued but may be as high as 25 cm. Surfaces lay an average of 65 cm above active channels and may be inset into unit **Qiag**. These deposits show little to moderate soil development, incipient to weak Av horizons as thick as 3 cm and weak to moderate cambic B horizon development (5 YR hue). Some late Pleistocene soils have Stage I to I+ pedogenic carbonate morphology, carbonate accumulations are also found at the alluvium/bedrock interface. Unit moderately to well vegetated with various perennial shrubs such as creosote bush (*Larrea tridentata*), white bur-sage (*Ambrosia dumosa*), several species of saltbush (*Atriplex sp),* and box thorn (*Lycium sp*.). Surface may be infrequently flooded during and after heavy rains. Drainage patterns are simple showing low relief. Diagnostic features: Grus-dominated deposits are found along granitic mountain fronts and pediments. These deposits are also found as terraces along younger to older channels and older young alluvial fans, they show no desert pavement or varnish development

Qiag **Intermediate-age alluvial fan deposit composed of grus (late and middle Pleistocene) –** Parent material is moderately to poorly sorted sand and silt derived from grus producing granite sources but may contain clasts from other lithologic sources. Deposits are characterized by surfaces abandoned for tens to hundreds of thousands of years. Poorly bedded to massive, moderately consolidated. Bar and swale micro-topography usually subdued. Surfaces lay an average of 160 cm above active channels (up to 5 m near active faults) and may be inset into unit **Qoag**. These deposits show moderate to strong soil development, Av horizons range from absent to moderately developed, moderate cambic B horizon development (7.5 to 5 YR hue). Older **Qiag** deposits have argillic Bt (to 2.5 YR hue) with angular, prismatic peds or may have eroded litter from exhumed calcic horizons. Some soils have Stage II to III+ pedogenic carbonate morphology, carbonate accumulations are found at the alluvium/bedrock interface. Unit is sparsely to moderately vegetated with various perennial shrubs such as creosote bush (*Larrea tridentata*), white bur-sage (*Ambrosia dumosa*), box thorn (*Lycium sp.),* and saltbush (*Atriplex sp.*), which appear to prefer carbonate-rich soils. Surface is rarely flooded during and after heavy rains. Diagnostic features: Grus-dominated deposits are found along granitic mountain fronts and pediments. Drainage patterns are distinct from **Qpi** incised pediment patterns

Qoag **Old alluvial fan deposit composed of grus (middle and early Pleistocene) –** Moderately to poorly sorted sand and silt derived from grus-producing granite sources but may contain clasts from other lithologic sources. Deposits are characterized by deeply incised fan remnants that have been abandoned for hundreds of thousands of years. Some **Qoag** deposits may result from localized reworking of materials derived from a deeply weathered pediment. Many surfaces have been stripped down to the well-indurated soil carbonate or are littered with carbonate debris. Poorly bedded to massive, well consolidated. Surfaces lay an average of 850 cm above active channels (up to 20 m near active faults). These deposits show strong soil development, some deposits show **Qiag** veneers. **Qoag** deposits have Stage IV and greater carbonate morphology, carbonate accumulations are found at the alluvium/bedrock interface. Unit is sparsely to moderately vegetated with various perennial shrubs such as creosote bush (*Larrea tridentata*), white bur-sage (*Ambrosia dumosa*), and box thorn (*Lycium sp)* which appears to prefer carbonate-rich soils. Surface is rarely flooded during and after heavy rains. Diagnostic features: Old grus-dominated deposits are found primarily on pediments. On aerial photographs, the drainage patterns are distinct from **Qpi** incised pediment patterns. Stage IV-VI pedogenic carbonate or carbonate litter usually exposed at the surface

Debris flow deposits

Qiad **Intermediate-age alluvial deposits (late and middle Pleistocene) –** dominated by debris flows. These deposits are classified by their hummocky topography

Eolian Deposits

Qae **Active eolian sand deposit (latest Holocene) –** Eolian sand deposits that are active and show evidence of migration. Composed of moderately to well-sorted sand and silt, loose; little or no soil development. Unit is sparsely vegetated with various perennial shrubs such as Joshua tree (*Yucca brevifolia*), creosote bush (*Larrea tridentata*), white bur-sage (*Ambrosia dumosa*), and saltbush (*Atriplex sp)*. Diagnostic features: Eolian deposits burying abandoned farmland or live shrubs

Qaed **Active eolian sand dune deposit (latest Holocene) –** Eolian sand dune deposits that are active and show evidence of migration

Qaes **Active eolian sand sheet deposit (latest Holocene) –** Eolian sand ramp deposits that are active and show evidence of migration

Qye **Young eolian deposit (Holocene and latest Pleistocene) –** Eolian sand deposits that are generally inactive. Composed of moderately to well-sorted sand and silt, sediments are loose. Little or no soil development but may show significant soil carbonate accumulation downwind of playas and dry lakes. Unit is sparsely vegetated with various perennial shrubs such as Joshua tree (*Yucca brevifolia*), creosote bush (*Larrea tridentata*), prickly pear (*Opuntia erinacea*), cholla (*Opuntia parishii* and *Opuntia acanthocarpa*), and saltbush (*Atriplex sp)*. Diagnostic features: Eolian deposits filling Qyw channels, burial of older deposits

Qyed **Young eolian sand dune deposit (Holocene and latest Pleistocene) –** Eolian sand dune deposits that are generally inactive

Qyer **Young eolian sand ramp deposit (Holocene and latest Pleistocene) –** Eolian sand ramp deposits that are generally inactive

Qyes **Young eolian sand sheet deposit (Holocene and latest Pleistocene) –** Eolian sand sheet deposits that are generally inactive

Mixed alluvial and eolian deposits

Qaea **Active mixed eolian and alluvial deposit (latest Holocene) –** mixed eolian and alluvial materials that show evidence of migration

Qyae **Young mixed alluvial and eolian fan deposit (Holocene and latest Pleistocene) –** mixed alluvial and eolian deposits that are generally inactive

Qyea **Young mixed eolian and alluvial deposit (Holocene and latest Pleistocene) –** mixed eolian and alluvial deposits that are generally inactive

Qiae **Intermediate-age mixed alluvial and eolian deposit (late and middle Pleistocene) –** dominated by alluvial processes. Forms flatter surfaces because the eolian deposits mute topographic relief with poor to moderate desert pavement development. Sand and gravelly sand displaying indistinct to well-defined thin bedding. Soil development is variable with weak to moderate cambic B horizons to weak argillic Bt horizons

Qiea **Intermediate-age mixed eolian and alluvial deposits (late and middle Pleistocene) –** dominated by alluvial processes. Forms flatter surfaces because the eolian deposits mute topographic relief with poor to moderate desert pavement development. Soil development is variable with weak to moderate cambic B horizons to weak argillic Bt horizons

Playa deposits

Qap **Active playa deposit (Holocene) –** Playa deposits that are active and have received sediment in the last few decades. Composed of fine sand, silt, and clay, salts may be present as efflorescences or as weak cements. Surfaces are flat and prone to flooding, surface water may pond on these low permeability materials. Sparsely vegetated to barren, vegetation such as iodine bush (*Allenrolfea occidentalis*), four-wing saltbush (*Atriplex canescens*), shadscale (*Atriplex confertifolia*) and hop-sage (*Grayia spinosa*) are found on playa fringes.

Qaps **Active sandy facies of playa deposit (Holocene) –** sandy playa deposits that are active and have received sediment in the last few decades

Qapf **Active playa fringe of mixed eolian, alluvial, lacustrine, ground-water discharge and playa deposits (Holocene) –** Active playa fringe that has received sediment in the last few decades. Diagnostic features: Flat, barren to sparsely vegetated, found along Qaw ephemeral stream channels or topographic low areas

Qyp **Young playa deposit (Holocene and latest Pleistocene) –** Playa deposits that are rarely flooded and may have received sediment in the last few centuries. Composed of fine sand, silt, and clay, salts may be present as efflorescences or as weak to moderate cements, weakly to moderately indurated; may show weak cambic B horizon development. Surfaces are flat and prone to flooding during heavy rains. Sparsely vegetated to barren, vegetation such as iodine bush (*Allenrolfea occidentalis*), four-wing saltbush (*Atriplex canescens*), shadscale (*Atriplex confertifolia*) and hop-sage (*Grayia spinosa*) are found on playa fringes.

Qyps **Young sandy facies of playa deposit (Holocene and latest Pleistocene) –** sandy playa deposits that are generally inactive

Qypf **Young playa fringe of mixed eolian, alluvial, lacustrine, ground-water discharge and playa deposits (Holocene and latest Pleistocene) –** Diagnostic features: Flat, barren to poorly vegetated, found along **Qyw** ephemeral stream channels or topographic low areas

Lacustrine deposits

Qil **Intermediate-age lacustrine deposit (late and middle Pleistocene) –** Complexly varying deposits of generally fine grain size, sand to silt, that are thin bedded in some cases and massive in others. Represents nearshore lake environments and distal alluvial fan environments modified by eolian erosion and deposition. Locally, discrete facies are mappable but generally, the unit is undividable. Soil development is similar to **Qia**. Differs from distal alluvial fan deposits by having very well sorted, thin-bedded sand and silt in places. Sparsely vegetated to barren; vegetation includes four-wing saltbush (*Atriplex canescens*), shadscale (*Atriplex confertifolia*) and hop-sage (*Grayia spinosa*)

Qilg **Intermediate-age lacustrine gravel deposit (late and middle Pleistocene) –** deposits of gravels generally associated with beaches and barrier bars

Qils **Intermediate-age lacustrine sand (late and middle Pleistocene) –** sandy lacustrine deposits that are inactive. Sparsely vegetated to barren; vegetation includes four-wing saltbush (*Atriplex canescens*), shadscale (*Atriplex confertifolia*) and hop-sage (*Grayia spinosa*)

Groundwater discharge deposits

Qygw **Young groundwater wetland deposit (Holocene and latest Pleistocene) –** Silt and fine sand, some groundwater carbonates, compact and thin-bedded to massive in zones of former groundwater discharge. Diagnostic features: Commonly forms light-colored badlands or flat areas. Sparsely vegetated to vegetated, vegetation includes four-wing saltbush (*Atriplex canescens*), shadscale (*Atriplex confertifolia*) and hop-sage (*Grayia spinosa*)

Qigw **Intermediate-age groundwater wetland deposit (late and middle Pleistocene)** – Silt and fine sand, some groundwater carbonates, compact and thin-bedded to massive in zones of former groundwater discharge. May overlie or intercalate with **Qia**, **Qoa**, **Qiag**, or **Qoag** deposits. Diagnostic features: Commonly forms light-colored badlands, abundant carbonate litter with root or stem casts. Sparsely vegetated to barren; vegetation includes four-wing saltbush (*Atriplex canescens*), shadscale (*Atriplex confertifolia*) and hop-sage (*Grayia spinosa*), with creosote bush (*Larrea tridentata*) and white bur-sage (*Ambrosia dumosa*) as minor components

Colluvial and landslide deposits

Qmc **Colluvial deposits (Holocene and Pleistocene)** – Hillslope materials thicker than 2 m and covering a wide area, generally poorly vegetated

Qyml **Young mass-movement deposit (Holocene) –** landslide deposits, thicker than 2 m that cover a wide area

Qiml **Intermediate-age mass-movement deposit (Pleistocene) –** landslide deposits, thicker than 2 m that cover a wide area. Present in the northwestern part of the mapping area

QTml **Extremely old landslide deposit (early Pleistocene and Pliocene) –** landslide deposit, thicker than 2 m, cemented with massive pedogenic carbonate. One deposit present 2 km east of the mouth of Red Rock Canyon

Hillslope deposits

Abundant hillslope deposits (Holocene and Pleistocene) – Hillslope materials such as colluvium, talus, and weathering products; covers more than 50% of the rock surface. Generally less than 2 m thick or of patchy distribution. Composed of:

Qha/ca	Abundant hillslope deposit overlying carbonate bedrock
Qha/fp	Abundant hillslope deposit overlying felsic plutonic bedrock
Qha/fpg	Abundant hillslope deposit overlying felsic plutonic bedrock that weathers to grus
Qha/fv	Abundant hillslope deposit overlying felsic volcanic bedrock
Qha/mp	Abundant hillslope deposit overlying mafic plutonic bedrock
Qha/mr	Abundant hillslope deposit overlying metamorphic bedrock
Qha/mv	Abundant hillslope deposit overlying mafic volcanic bedrock
Qha/pc	Abundant hillslope deposit overlying partly consolidated bedrock
Qha/sc	Abundant hillslope deposit overlying schistose bedrock
Qha/sl	Abundant hillslope deposit overlying siliciclastic bedrock

Sparse hillslope deposits (Holocene and Pleistocene) – Hillslope materials such as colluvium, talus, and weathering products; covers less than 50% of the rock surface. Generally less than 2 m thick or of patchy distribution. Composed of:

Qhs/ca	Sparse hillslope deposit overlying carbonate bedrock
Qhs/fp	Sparse hillslope deposit overlying felsic plutonic bedrock
Qhs/fpg	Sparse hillslope deposit overlying carbonate bedrock that weathers to grus
Qhs/fv	Sparse hillslope deposit overlying felsic volcanic bedrock
Qhs/mp	Sparse hillslope deposit overlying mafic plutonic bedrock
Qhs/mr	Sparse hillslope deposit overlying metamorphic bedrock
Qhs/mv	Sparse hillslope deposit overlying mafic volcanic bedrock
Qhs/sc	Sparse hillslope deposit overlying partly consolidated bedrock
Qhs/sl	Sparse hillslope deposit overlying siliciclastic bedrock

Pediment surface

Pediment surfaces (Holocene and Pleistocene) – Erosional surfaces in various stages of erosion or aggradation. Divided into three classes by surface characteristics. **Qpv**, veneer of sediment, generally less than 2 m thick, is present on the pediment. Pediment veneer deposits can show soil development similar to **Qyag**, **Qyaog**, **Qiag**, or **Qoag**; **Qpi**, incised pediment with most of the pediment expressed as a surface of exposed rock; **Qpd**, deeply dissected pediment identified by pinnacles, ridges, or other bedrock remnants of similar height

Qpv-fpg	Pediment in felsic plutonic rocks with veneer of grus
Qpv-mp	Pediment in mafic plutonic rocks with veneer of sediment
Qpi-fp	Incised pediment in felsic plutonic rocks
Qpi-fpg	Incised pediment in felsic plutonic rocks that weather to grus
Qpi-mp	Incised pediment in mafic plutonic rocks
Qpd-fp	Deeply dissected pediment in felsic plutonic rocks
Qpd-fpg	Deeply dissected pediment in felsic plutonic rocks that weather to grus
Qpd-mp	Deeply dissected pediment in mafic plutonic rocks

Composite symbols

Surficial geologic units may be found as thin (<2 m) veneers over older units. In areas where this relationship is common, the unit designators are shown on the map separated by a slash (/). For example, Qya/Qia indicates a veneer of young alluvial fan deposits over intermediate-age alluvial fan deposits and Qye/mv shows a young eolian deposit over mafic volcanic rocks. The extent of individual deposits is commonly small enough that each deposit cannot be shown individually at the published map scale. For example, Qaa + Qyao indicate an area where deposits of both Qaa and Qyao are found and Qaa is more common.

Bedrock substrate materials

Carbonate rocks [ca] – Carbonate mineral rocks such as limestone, dolomite, and marble

Felsic plutonic rocks [fp] – Plutonic rocks with more than about 68% SiO_2, such as granite and granodiorite

Felsic plutonic rocks that weather to grus [fpg] – felsic plutonic rocks that weather to grus

Felsic volcanic rocks [fv] – Volcanic rocks with more than about 68% SiO_2, such as rhyolite, dacite, rhyodacite ,and felsite, including flows and ejecta

Mafic plutonic rocks [mp] – Plutonic rocks with less than about 68% SiO_2, such as gabbro, diorite, monzodiorite, syenite, and alkalic rocks
Metamorphic rocks [mr] – Metamorphic rocks of complexly mixed lithology, such as gneiss, migmatite, and structurally mixed rocks

Mafic volcanic rocks [mv] – Volcanic rocks with less than about 68% SiO_2, such as andesite, and basalt, including flows and ejecta

Partly consolidated [pc] – weakly to moderately consolidated sedimentary deposits, volcanic ejecta, or highly altered rocks; typically middle to late Tertiary age

Schistose rocks [sc] – schist, phyllite, and other mica-rich rocks

Siliclastic rocks [sl] – Silicic sedimentary and metamorphic rocks, such as sandstone, quartzite, shale, and siltstone

References:

Aydin, A., and Nur, A., 1982, Evolution of pull-apart basins and their scale independence: Tectonics, v. 1, p. 91-105.

Birkeland, P.W., 1999, Soils and Geomorphology: New York, Oxford University Press, 430 p.

Birkeland, P.W., Machette, M.N., and Haller, K.M., 1991, Soils as a Tool for Applied Quaternary Geology: Salt Lake City, UT, Utah Geological and Mineral Survey, 63 p.

Boettinger, J.L., and Southard, R.J., 1991, Silica and carbonate sources for Aridisols on a granitic pediment, western Mojave Desert: Soil Science Society of America Journal, v. 55, p. 1057-1067.

—, 1995, Phyllosilicate distribution and origin in Aridisols on a granitic pediment, western Mojave Desert: Soil Science Society of America Journal, v. 59, p. 1189-1198.

Bryant, W.A., 1987, Recently active traces of the Blackwater, Harper, Lockhart and related faults near Barstow, San Bernardino County, California Division of Mines and Geology, p. 17, 7 plates at various scales.

Burke, D.B., Hillhouse, J.W., McKee, E.H., Miller, S.T., and Morton, J.L., 1982, Cenozoic rocks of the Barstow Basin area of Southern California - Stratigraphic relations, radiometric dates, and paleomagnetism: Washington, D.C., U.S. Geological Survey, Bulletin 1529-E, p. 16.

Carr, M.D., Christiansen, R.L., and Poole, F.G., 1997, Bedrock geologic map of the El Paso Mountains in the Garlock and El Paso Peaks 7 1/2' quadrangles, Kern County, California: Washington, D.C., U.S. Geological Survey, Miscellaneous Investigations Series Map I-2389, scale 1:24,000.

Carr, M.D., Harris, A.G., Poole, F.G., and Fleck, R.J., 1993, Stratigraphy and structure of the Paleozoic outer continental margin rocks in Pilot Knob Valley: Washington, D.C., U.S. Geological Survey Bulletin 2015, p. 33.

Carter, B.A., 1980, Quaternary displacement on the Garlock fault, California, *in* Fife, D.L., and Brown, A.R., eds., Geology and Mineral Wealth of the California Desert: Santa Ana, CA, South Coast Geological Society, p. 457-466.

—, 1994, Neogene offsets and displacement rates, central Garlock fault, California, *in* McGill, S.F., and Ross, T.M., eds., Geological Investigations of an active margin, 1994 G.S.A. Cordilleran Section Guidebook: Boulder, CO, Geological Society of America, p. 345-364.

Carter, J.N., Luyendyk, B.P., and Terres, R.R., 1987, Neogene clockwise tectonic rotation of the eastern Transverse Ranges, California, suggested by paleomagnetic vectors: Geological Society of America Bulletin, v. 98, p. 199-207.

Clark, M.M., 1973, Map showing recently active breaks along the Garlock and associated faults, California: Washington, D.C., U.S. Geological Survey, Miscellaneous Geologic Investigations Map I-741.

Cooke, R.U., and Mason, P.F., 1973, Desert Knolls pediment and associated landforms in the Mojave Desert, California: Revue de geomorphologie dynamique, v. 22, p. 49-60.

Cooke, R.U., and Warren, A., 1973, Geomorphology in Deserts: Berkeley, University of California Press, 374 p.

Cox, B.F., and Diggles, M.F., 1986, Geologic map of the El Paso Mountains Wilderness study area, Kern County, California: Washington, D.C., U.S. Geological Survey, Miscellaneous Field Studies Map MF-1827, scale 1:24,000.

Davis, G.A., and Burchfiel, B.C., 1973, Garlock fault: an intracontinental transform structure: Geological Society of America Bulletin, v. 84, p. 1407-1422.

Dibblee, T.W., 1952, Geology of the Saltdale quadrangle, California: San Francisco, CA, California Division of Mines Bulletin 160, p. 43.

—, 1967, Areal Geology of the Western Mojave Desert, California: Washington, D.C., U.S. Geological Survey Professional Paper 522, p. 153, with 4 plates, scale 1:125,000.

—, 1968, Geology of the Fremont Peak and Opal Mountain quadrangles, California: Sacramento, CA, California Division of Mines and Geology, Bulletin 188, p. 64, four plates, scale 1:62,500.

—, 1985, Analysis of potential fault and seismic hazards to proposed Superconductor Supercollider site in vicinity of Edwards Air Force Base, western Mojave Desert, California, unpublished report for University of California at Davis, p. 12.

Dibblee, T.W., and Gay, T.E., 1952, Mineral deposits of the Saltdale quadrangle [California]: San Francisco, CA, California Division of Mines, Bulletin 160, p. 45-64.

Dohrenwend, J.C., Wells, S.G., McFadden, L.D., and Turrin, B.D., 1986, Pediment dome evolution in the eastern Mojave Desert, *in* Gardiner, V., ed., International geomorphology, 1986 : proceedings of the First International Conference on Geomorphology: London, Wiley-Interscience, p. 1047-1062.

Dokka, R.K., 1989, The Mojave Extensional Belt of southern California: Tectonics, v. 8, p. 363-390.

Dokka, R.K., and Travis, C.J., 1990, Late Cenozoic strike-slip faulting in the Mojave Desert, California: Tectonics, v. 9, p. 311-340.

Eghbal, M.K., and Southard, R.J., 1993a, Micromorphological evidence of polygenesis of three Aridisols, western Mojave Desert, California: Soil Science Society of America Journal, v. 57, p. 1041-1050.

—, 1993b, Stratigraphy and genesis of Durothids and Haplargids on dissected alluvial fans, western Mojave Desert, California: Geoderma, v. 59, p. 151-174.

Fletcher, J.M., 1994, Geodynamics of large-magnitude extension: A field-based study of the central Mojave metamorphic core complex [Ph.D. thesis]: Salt Lake City, University of Utah.

Fletcher, J.M., Bartley, J.M., Martin, M.W., Glazner, A.F., and Walker, J.D., 1995, Large-magnitude continental extension: An example from the central Mojave metamorphic core complex: Geological Society of America Bulletin, v. 107, p. 1468-1483.

Fletcher, J.M., Miller, J.S., Martin, M.W., Boettcher, S.S., Glazner, A.F., and Bartley, J.M., 2002, Cretaceous arc tectonism in the Mojave block: Profound crustal modification that controlled subsequent tectonic regimes, *in* Glazner, A.F., Walker, J.D., and Bartley, J.M., eds., Geologic Evolution of the Mojave Desert and Southwestern Basin and Range: Boulder, CO, Geological Society of America Memoir 195, p. 131-149.

Gale, H.S., 1946, Geology of the Kramer borate district, Kern County, California: California Journal of Mines and Geology, v. 42, p. 325-378.

Glazner, A.F., Walker, J.D., Bartley, J.M., Fletcher, J.M., Martin, M.W., Schermer, E.R., Boettcher, S.S., Miller, J.S., Fillmore, R.P., and Linn, J.K., 1994, Reconstruction of the Mojave Block, *in* Ross, T.M., ed., Geological Investigations of an active margin, Geological Society of America Cordilleran Section Guidebook: Redlands, CA, San Bernardino County Museum Association, p. 3-30.

Gile, L.H., Hawley, J.W., and Grossman, R.B., 1981, Soils and geomorphology in the Basin and Range area of Southern New Mexico - Guidebook to the Desert Project: Socorro, NM, New Mexico Institute of Mining and Technology, 222 p.

Hewett, D.F., 1954a, A fault map of the Mojave Desert region [California], *in* Jahns, R.H., ed., Geology of southern California: Sacramento, CA, California Division of Mines, Bulletin 170, p. 15-18, 1 plate.

—, 1954b, General geology of the Mojave Desert region, California, [part]1, *in* Jahns, R.H., ed., Geology of southern California: Sacramento, CA, California Division of Mines, Bulletin 170, p. 5-20.

Hulin, C.D., 1925, Geology and oil resources along the southern border of San Joaquin Valley, California: Sacramento, CA, California Mining Bureau, Bulletin 95, p. 152.

Jennings, C.W., Burnett, J.L., and Troxel, B.W., 1962, Geologic Map of California - Trona Sheet, 1:250,000: San Francisco.

Keenan, D.L., 2000, The geology and geochemistry of volcanic rocks in the Lava Mountains, California [M.S. thesis]: Las Vegas, University of Nevada.

Loomis, D.P., 1984, Miocene stratigraphic and tectonic evolution of the El Paso Basin, California [M.S. thesis]: Chapel Hill, NC, University of North Carolina.

Loomis, D.P., and Burbank, D.W., 1988, The stratigraphic evolution of the El Paso basin, southern California: Implications for Miocene development of the Garlock fault and uplift of the Sierra Nevada: Geological Society of America Bulletin, v. 100, p. 12-28.

Louie, J.N., and Qin, J., 1991, Subsurface imaging of the Garlock fault, Cantil Valley, California: Journal of Geophysical Research, v. 96, p. 14,461-14,479.

Mabey, D.R., 1960, Gravity survey of the western Mojave Desert, California: Washington, D.C., U.S. Geological Survey, Professional Paper 316-D, p. 51-73.

Machette, M.N., 1985, Calcic soils of the southwestern United States, *in* Weide, D.L., ed., Soils and Quaternary geology of the southwestern United States, Volume Special Paper 203: Boulder, CO, Geological Society of America, p. 1-22.

McGill, S., and Rockwell, T., 1998, Ages of late Holocene earthquakes on the central Garlock fault near El Paso Peaks, California: Journal of Geophysical Research, v. 103, p. pp. 7265-7279.

McGill, S., and Sieh, K., 1991, Surficial offsets on the central and eastern Garlock fault associated with prehistoric earthquakes: Journal of Geophysical Research, v. 96, p. pp. 21, 597-21,621.

—, 1993, Holocene slip rate of the central Garlock fault in southeastern Searles Valley, California: Journal of Geophysical Research, v. 98, p. pp. 14,217-14,231.

McGill, S.F., Anderson, H., Daneke, T., Grant, J., Slates, M., Stroud, J., Tegt, S.K., and McGill, J.D., 2003, Slip rate of the western Garlock fault near Lone Tree Canyon, Mojave Desert, California: Geological Society of America, Abstracts with Programs, v. 35, p. 64.

Michael, E.D., 1966, Large lateral displacement on the Garlock fault, California, as measured from offset fault system: Bulletin of the Geological Society of America, v. 77, p. 111-114.

Miller, D.M., and Yount, J.C., 2002, Late Cenozoic tectonic evolution of the north-central Mojave Desert inferred from fault history and physiographic evolution of the Fort Irwin area, California, *in* Bartley, J.M., ed., Geologic Evolution of the Mojave Desert and Southwestern Basin and Range: Boulder, CO, Geological Society of America, Memoir 195, p. 173-197.

Monastero, F.C., Sabin, A.E., and Walker, J.D., 1997, Evidence for post-early Miocene initiation movement on the Garlock fault from offset of the Cudahy Camp Formation, east-central California: Geology, v. 25, p. 247-250.

Oberlander, T.M., 1989, Slope and pediment systems, *in* Thomas, D.S.G., ed., Arid Zone Geomorphology: London, Belhaven Press, p. 56-84.

Oskin, M., and Iriondo, A., 2004, Large-magnitude transient strain accumulation on the Blackwater fault, Eastern California shear zone: Geology, v. 32, p. 313-316.

Pack, R.W., 1914, Reconnaissance of the Barstow-Kramer region, California: Washington, D.C., U.S. Geological Survey, Bulletin 541-E, p. 141-154.

Page, P.W., and Moyle, J., W.R., 1960, Data on water wells in the eastern part of the middle Mojave Valley area, San Bernardino County, California, California Department of Water Resources, Bulletin No. 91-19, p. 223, 1 plate, scale 1:62,500.

Pampeyan, E.H., Holzer, T.L., and Clark, M.M., 1988, Modern ground failure in the Garlock fault zone, Fremont Valley, California: Geological Society of America Bulletin, v. 100, p. 677-691.

Peltzer, G., Crampe, F., Hensley, S., and Rosen, P., 2001, Transient strain accumulation and fault interaction in the Eastern California Shear Zone: Geology, v. 29, p. 975-978.

Reynolds, R.E. and Fay L.P., 1989, The Coon Canyon Fault crevice local fauna: Preliminary evidence for recency of faulting in the Mud Hills, San Bernardino County, California, in Reynolds, R.E. ed., The west-central Mojave Desert: Quaternary studies between Kramer and Afton Canyon: Redlands CA, San Bernardino County Museum Association Special Publication, 89, p. 61-64.

Rowlands, P.G., 1995, Regional bioclimatology of the California Desert, *in* Latting, J., and Rowlands, P.G., eds., The California Desert: An Introduction to Natural Resources and Man's Impact: Riverside, CA, University of California, Riverside Press, p. 95-134.

Schell, B.A., 1994, Newly discovered faults along the northwest extension of the Lockhart fault zone, Mojave Desert, Kern County, California, *in* Murbach, D., and Baldwin, J., eds., Mojave Desert: Santa Ana, CA, South Coast Geological Society, p. 239-252.

Smith, E.I., Sanchez, A., Keenan, D.L., and Monastero, F.C., 2002, Stratigraphy and geochemistry of volcanic rocks in the Lava Mountains, California: Implications for the Miocene development of the Garlock Fault, *in* Glazner, A.F., Walker, J.D., and Bartley, J.M., eds., Geologic Evolution of the Mojave Desert and Southwestern Basin and Range: Boulder, CO, Geological Society of America, Memoir 195, p. 151-160.

Smith, G.I., 1964, Geology and volcanic petrology of the Lava Mountains, San Bernardino County, California: Washington, D.C., U.S. Geological Survey Professional Paper 457, p. 97, 1 sheet, 1: 24, 000.

—, 1991, Anomalous folds associated with the east-central part of the Garlock fault, southeast California: Geological Society of America Bulletin, v. 103, p. 615-624.

Thompson, 1929, The Mohave Desert region, California: USGS Water Supply Paper 578, 759 p.

Troxel, B.W., and Morton, P.K., 1962, Geologic Map of Kern County: San Francisco, California Division of Mines and Geology, scale 1:250,000.

Westaway, R., 1995, Deformation around stepovers in strike-slip fault zones: Journal of Structural Geology, v. 17, p. 831-846.

Yount, J.C., Schermer, E.R., Felger, T.J., Miller, D.M., and Stephens, K.A., 1994, Preliminary geologic map of Fort Irwin Basin, north-central Mojave Desert, California, U.S. Geological Survey Open-File Report 94-173, 1:24,000 scale, 27 p.